Nanosilica as Dry Bonding System Component and as Reinforcement in Short Nylon-6 Fiber/Natural Rubber Composite

Leny Mathew,[1,2] Sunil K. Narayanankutty[1]

[1]*Department of Polymer Science and Rubber Technology, Cochin University of Science and Technology, Kochi-682 022, India*
[2]*Department of Polymer Engineering, Mahatma Gandhi University College of Engineering, Thodupuzha-685 587, Kerala, India*

Received 7 December 2007; accepted 11 November 2008
DOI 10.1002/app.29718
Published online 13 February 2009 in Wiley InterScience (www.interscience.wiley.com).

ABSTRACT: Nanoscale silica was synthesized by acid hydrolysis of sodium silicate using dilute hydrochloric acid under controlled conditions. The synthesized silica was characterized by SEM, BET adsorption, and XRD. The particle size of silica was calculated to be 13 nm from the XRD results and the surface area was found to be 295 m^2/g by BET method. This synthesized nanosilica was used in place of conventional silica in HRH (hexamethylenetetramine, resorcinol and silica) bonding system for natural rubber/Nylon-6 short fiber composite. Nanosilica was also used as reinforcing filler in natural rubber/Nylon-6 short fiber hybrid composite. Mechanical, thermal, and dynamic mechanical properties of the composites were evaluated. The introduction of the nanosilica in hybrid composites improved the tensile strength, modulus, and tear strength through improved interaction with the matrix which is facilitated by the higher surface area. Abrasion loss and hardness were also better for the nanosilica composites. Resilience and compression set were adversely affected. The hybrid composites showed anisotropy in mechanical properties. Peak rate of thermal decomposition decreased and temperature of initiation of thermal degradation increased with silica content, indicating improved thermal stability of the hybrid composites. The storage modulus and loss modulus showed two-stage dependence on frequency at higher fiber loading.
 J Appl Polym Sci 112: 2203–2212, 2009

Key words: composite; fibers; nylon; silica; rubber

INTRODUCTION

Short fiber reinforced composites are finding ever-increasing applications in engineering and consumer products. Short fibers are used to improve or modify certain thermo mechanical properties of the matrix for specific applications or to reduce the cost of the fabricated article. Because short fibers can be incorporated directly into the rubber compound along with other additives, the resulting composites are amenable to the standard rubber processing steps of extrusion, calendering and the various type of molding operations such as compression, injection and transfer molding. These composites find application in most general purpose and speciality products ranging from belts, hoses, diaphragms and seals to tires. The degree of reinforcement by short fibers is governed largely by the following characteristics: fiber concentration, fiber aspect ratio, fiber adhesion to the matrix, fiber orientation and its dispersion in the matrix.[1–6]

Correspondence to: S. K. Narayanankutty (sunil@cusat.ac.in).

Journal of Applied Polymer Science, Vol. 112, 2203–2212 (2009)

Fiber-matrix adhesion in short fiber rubber composites has been a field of extensive research.[7–12] In the case of short fiber reinforced rubber composites, the load is not directly applied to the fiber; rather, it is applied to the matrix. To obtain a high performance composite, the load must be effectively transferred to the fiber, which is possible only when the fiber-matrix interface is strong. The adhesion between the fiber and the matrix should be such that the failure occurs in the matrix rather than at the interface.[13–17] The conventional method for improving the fiber-matrix bond has been the use of a dipping solution based on rubber latex and a polymeric resin. But compared with this adhesive dipping process, the use of a tricomponent dry bonding system consisting of hexamethylenetetramine, resorcinol and fine particle hydrated silica (HRH system) is easier. This is because, the constituents of the dry bonding system can be added to the rubber matrix like any other compounding ingredient and additional processes like dipping and drying can be avoided. Dunnom[18] observed a marked difference in the adhesion between the matrix and the fiber by adding silica to a compound containing resorcinol and hexa. Rajeev et al.,[8] Sreeja and Kutty,[11] Derringer,[19] Murty and De[20] and De and coworkers[21] have described the

various aspects of short fiber adhesion to rubber in the presence of the dry bonding system. In all these studies they have used conventional precipitated silica with particle size in microns.[8,19,21–24] As the role of silica is to improve wetting of the fiber surface,[18–20,23] silica with smaller particle size can be more effective in improving wettability of the fibers. Recently, Tapasikotoky and Dolui,[25] Jerzy Chrusoid and Ludomir Slusaraski[26] have reported the preparation of silica with particle size in the nanometer range. In this work we report the effect of nanosilica as a component of the HRH dry bonding system and also as a filler in short Nylon-6/natural rubber composites. The mechanical, thermal and dynamic mechanical properties of nanosilica/Nylon-6 short fiber/natural rubber hybrid composites are presented

EXPERIMENTAL

Materials used

Natural rubber used in this study was ISNR-20, obtained from R.R.I.I, Kottayam, India. Nylon fiber (N6) obtained from SRF, Chennai, India, was chopped to approximately 6 mm length. Zinc oxide, stearic acid, *N*-(1,3-dimethylbutyl)*N*′-phenyl-*p*-phenylenediamine (6PPD), *N*-cyclohexyl-2-benzothiazole sulfenamide (CBS), tetramethyl-thiuramdisulphide (TMTD), sulfur, hexamethylenetetramine (Hexa) and resorcinol used were of commercial grade.

TABLE I
Formulation of Mixes

		Ingredients (phr)[a]			
Mix no.		Nylon-6	Nanosilica	Commercial silica	HRH[b]
A series	A_0	–	–	–	–
	A_{10}	10	–	–	1.67
	A_{20}	20	–	–	3.33
	A_{30}	30	–	–	5
B series	B_0	–	3	–	–
	B_{10}	10	3	–	1.67
	B_{20}	20	3	–	3.33
	B_{30}	30	3	–	5
C series	C_0	–	6	–	–
	C_{10}	10	6	–	1.67
	C_{20}	20	6	–	3.33
	C_{30}	30	6	–	5
D series	D_0	–	9	–	–
	D_{10}	10	9	–	1.67
	D_{20}	20	9	–	3.33
	D_{30}	30	9	–	5
E series	E_0	–	–	6	–
	E_{10}	10	–	6	1.67
	E_{20}	20	–	6	3.33
	E_{30}	30	–	6	5

Natural rubber-100 phr, Zinc oxide-5 phr, Stearic acid-2 phr, N-(1,3- dimethylbutyl)N′-phenyl-p-phenylenediamine) -1 phr, CBS-0.6 phr, TMTD- 0.2 phr, and sulphur-2.5 phr were common to all mixes.

[a] phr, parts per hundred rubber.

[b] Hexa : Resorcinol : Silica in the ratio 2 : 2 : 1. Total loading was 16% on fiber content.

Synthesis of nanosilica

Nanosilica was synthesized by acid hydrolysis of sodium silicate using dilute hydrochloric acid as suggested by Taposikotoky and Dolui.[25] Sodium silicate is a cost effective silica source as compared with the more commonly used tetraethoxysilane (TEOS) or tetramethoxysilane (TMOS).[26] Moreover, by using a purely aqueous medium, the expensive and very often toxic solvent could be avoided.

Fifteen percent sodium silicate solution was prepared with 1% polyvinyl alcohol solution. Then, 0.5*N* HCl, was added to it slowly with stirring at a temperature of 60°C. The pH of the mixture was maintained between 1and 2. The solution was stirred at 60°C for 30 min to carry out acid hydrolysis of sodium silicate. The sol-gel mixture was then washed well to remove all the sodium chloride formed. It was dried at 50°C and then muffled at 600°C.

Characterization of nanosilica

Scanning electron microscopy

The prepared silica surfaces were sputter coated with gold and examined under scanning electron microscopy (SEM) Model No. S 360 Cambridge Instruments, U. K. The tensile and tear fracture surfaces were also sputter coated with gold and examined under the same Scanning Electron Microscope.

X-ray diffraction

The x-ray diffraction (XRD) analysis was performed with X-Ray Diffractometer, Bruker, D8 Advance model, employing CuKa radiation ($\lambda = 1.54$ Å) and Ni filter operating at 30 kV and 20 mA.

BET adsorption

Surface area of the silica was determined by the BET method using nitrogen isotherm on a Micromeritics Tristar 3000, surface area and porosity analyzer.

Preparation of the composites

The formulation of mixes is given in Table I. The mixing was performed as per ASTM D-3184 (1989) standard on a two-roll laboratory size mixing mill (150×300 mm^2). Nylon-6 fibers were added in

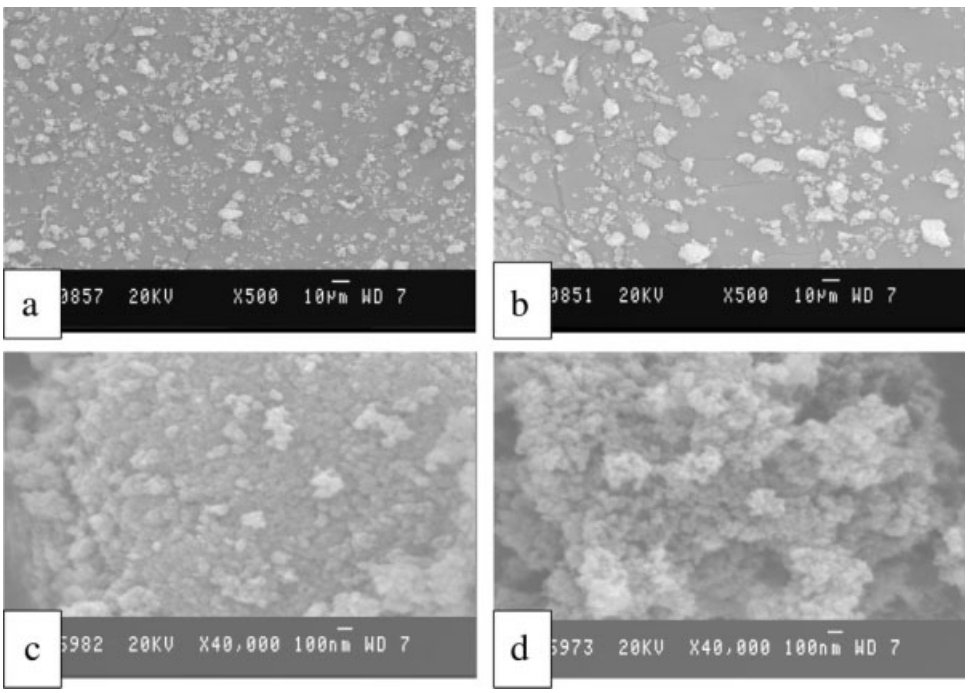

Figure 1 (a) and (c) SEM picture of synthesized nanosilica, (b) and (d) SEM picture of commercial silica.

small increments to obtain uniform dispersion. After complete mixing, the stock was finally sheeted out through tight nip so as to orient the fibers in one direction. The thin sheet obtained was cut in the required dimension and stacked one above the other to the desired volume. The sheets were vulcanized in the hydraulic press at 150°C and 200 kg/cm^2 pressure to their optimum cure times as determined using a Rubber Process Analyzer (RPA–2000), Alpha Technology.

Measurement of physical properties

The tensile properties were measured using Shimadzu Universal Testing Machine model AG -1, 10 kN according to ASTM D 412 standard at a crosshead speed of 500 mm/min. Test specimens were punched out, with fibers oriented along the milling direction (longitudinal) and across the milling direction (transverse) for testing the mechanical properties. The tear strength was determined according to ASTM D 624 (Die C). The hardness (Shore A) was determined as per ASTM D2240-86 using a Zwick 3114 hardness tester. Abrasion resistance of the samples was measured using an abrader based on DIN 53516. Rebound resilience was determined by the vertical rebound method according to ASTM D 2832-88. Compression set at constant strain was measured according to ASTM D 395-86 method B.

Volume fraction of rubber, V_r

V_r of the samples was determined from the equilibrium swelling data using the equation

$$V_r = \frac{(D - FT)\rho_r^{-1}}{(D - FT)\rho_r^{-1} + A_0\rho_s^{-1}}$$

where D is the de-swollen weight of the sample, F is the weight fraction of the insoluble component, T is the initial weight of the sample, ρ_r is the density of the rubber, ρ_s is the density of the solvent, and A_o is the weight of solvent absorbed.

Here, $\rho_r = 0.92$ g/cc and solvent used was toluene with $\rho_s = 0.886$ g/cc.

Thermal analysis

Thermo gravimetric analysis of the composites was performed in a Q20 Thermo Gravimetric Analyzer, TA Instruments at a heating rate of 10°C/min from room temperature to 800°C under nitrogen atmosphere.

Dynamic mechanical analysis

The dynamic mechanical thermal analysis was conducted using rectangular test specimens having a dimension of 30 × 5 × 2 mm^2 were tested under

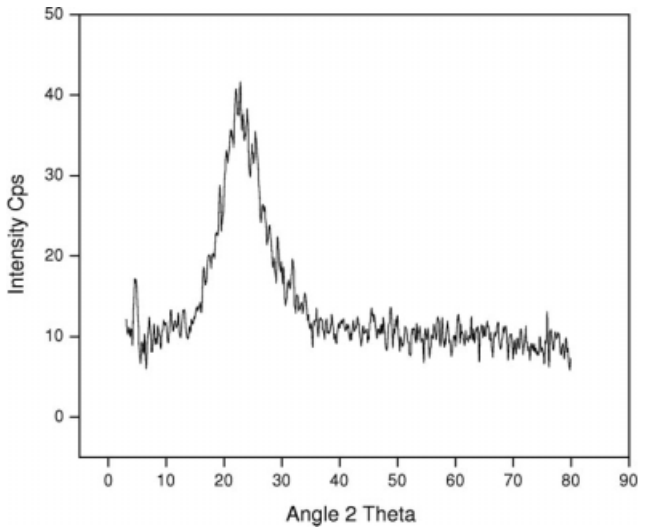

Figure 2 XRD pattern of synthesized nanosilica.

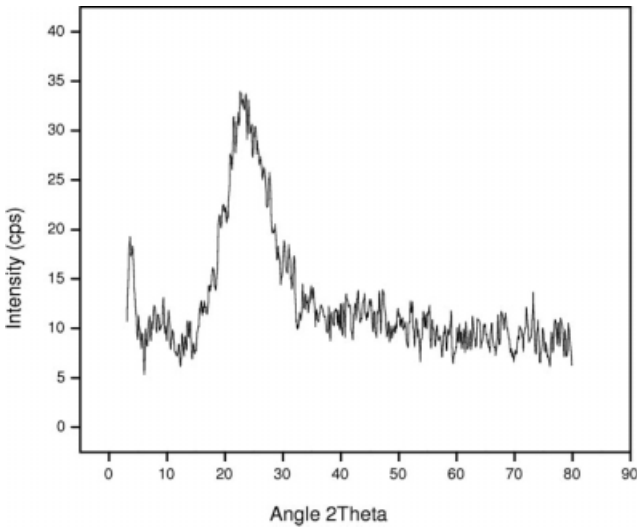

Figure 3 XRD pattern of commercial silica.

tension mode using a TA Instruments DMA Q-800 at a constant temperature of 70°C. The frequency was varied from 1 to 50 Hz under frequency sweep mode at a rate of 2 Hz/min. The samples were subjected to dynamic tension strain amplitude of 0.1146%.

RESULTS AND DISCUSSION

Characterization of nanosilica

Scanning electron microscopy

Figure 1(a,b) show the SEM photographs of the synthesized silica and commercially available silica, respectively. These pictures show that the synthesized silica has lower particle size than the commercial silica. The small particle size provides large external surface area, which results in improved in the mechanical properties. Figure 1(c,d) are the SEM of nanosilica and commercial silica respectively, at 40,000× magnification. It is seen that both the silica are of nanometer size. In the case of commercial silica the particles are agglomerated to a larger extent.

X-ray diffraction studies

X-ray diffraction patterns of the two types of silica are shown in Figures 2 and 3. Both the figures shows similar pattern with major peak at $2\theta = 22.08^\circ$. The full width at half maximum (β) is, however different for the two type of the silica. The β is used to determine the particle size using the Debye-Sherrer formula

$$C_s = 0.9\lambda/\beta\cos\theta$$

where, C_s is the particle size, λ is the wavelength of the incident x-ray beam, β is the full width at half maximum (FWHM) of the X-ray diffraction peaks and θ is half of the angle 2θ corresponding to the peak. The average particle size, C_s, of the prepared silica is found to be 13 nm and that of the commercial silica is 34 nm.

BET adsorption

Table II gives the BET adsorption results of the synthesized silica and that of commercial silica. The surface area of the synthesized silica is found to be 295 m^2/g and that of commercial silica is 178 m^2/g. From this it is clear that synthesized silica has higher surface area than that of commercial silica.

Mechanical properties

Figure 4 gives the variation of tensile strength with fiber loading for mixes containing silica in the range 0–9 phr. The tensile strength increases with fiber content with an initial minor drop at 10 phr fiber loading. This pattern is characteristic of any strain - crystallising matrix such as natural rubber.[27,28] The presence of fibers in such matrices leads to two simultaneous phenomena–one the dilution effect due to its physical presence and two the reinforcement effect due to its interaction with the matrix. At lower loadings, because the first effect is more significant, the ultimate strength is lowered. However, as the fiber content increase, the reinforcement effect takes

TABLE II
Surface Area of the Silica Samples

Samples	Surface area (m^2/g)
Synthesized silica	295
Commercial silica	178

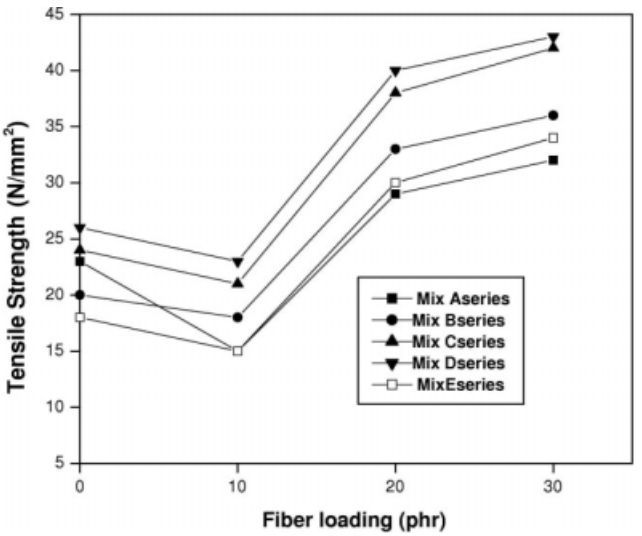

Figure 4 Variation of tensile strength with fiber loading in longitudinal direction.

over and results in much improvement in the tensile strength.

At any fiber content the tensile strength is higher in the presence of nanosilica. For the gum compound (mix A_0) the tensile strength is improved by 13% with just 6 phr of nanosilica. For the fiber filled samples also the tensile strength is improved in the presence of nanosilica. For the 30 phr fiber loaded samples the tensile strength is improved by 40% in the presence of 6 phr of nanosilica. As the percentage improvement is higher in the case of fiber loaded samples, silica may be contributing positively to the interaction of the fibers with the matrix. Silica is also known to improve the wetting of short fibers in natural rubber matrix.[28] Series E is the mixes containing 6 phr of conventional silica instead of nanosilica. It shows tensile strength values almost equal to the mixes without silica (Series A). This implies that the nanosilica has better interaction with the matrix and hence improves wettability of the short fibers, resulting in higher tensile strength.

SEM studies of the tensile fractured samples also support this view. Figure 5(a,b) show the tensile fracture surfaces of Mixes C_{10} and C_{30}, respectively. Fiber surface is not smooth. Matrix is adhered on to the fiber surface. Fiber ends are seen to be broken. This indicates that there is a strong bond existing between the fiber and the matrix. Figure 5(c,d) are the micrographs of the tensile fracture surface of samples containing commercial silica (Mixes E_{10} and E_{30}, respectively). The fibers are pulled out from the matrix. No matrix is adhered on to the fiber surface as the bond is not as strong as in the case of nanosilica.

For the samples with fibers oriented in the transverse direction (fibers oriented perpendicular to the direction of application of force), the variation is shown in Figure 6. In all the cases, the tensile strength drops to a very low value and shows only a marginal recovery at 30 phr of fiber loading. With increasing silica content (Series A-E), the improvement is also very limited. Series containing 9 phr of nanosilica (Series D) shows the highest tensile

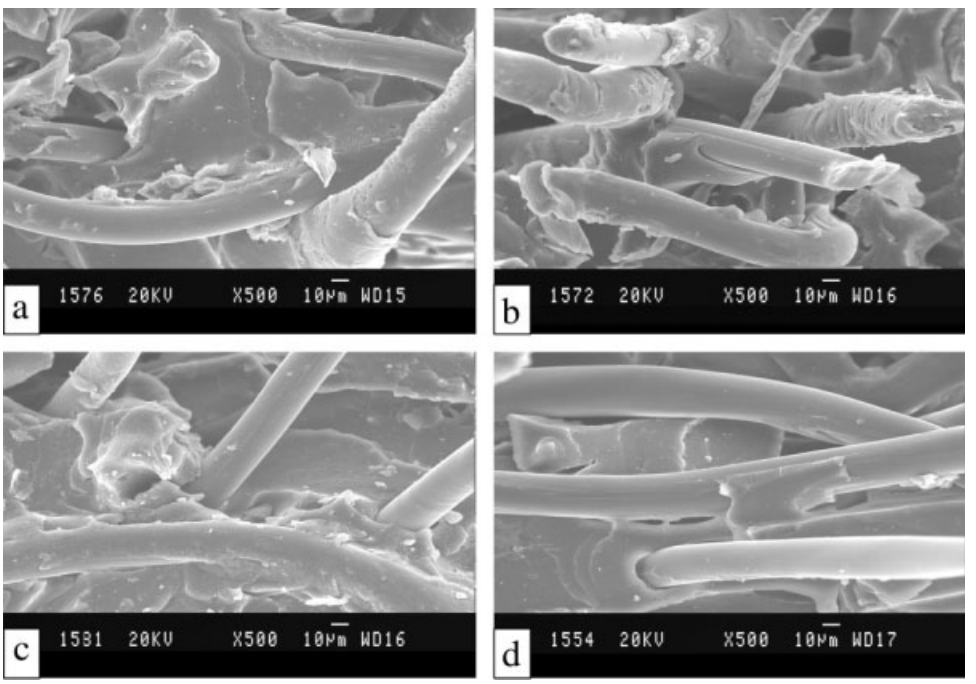

Figure 5 Scanning electron micrographs of (a) Mix C_{10}, (b) Mix C_{30},(c) Mix E_{10}, and (d) Mix E_{30}.

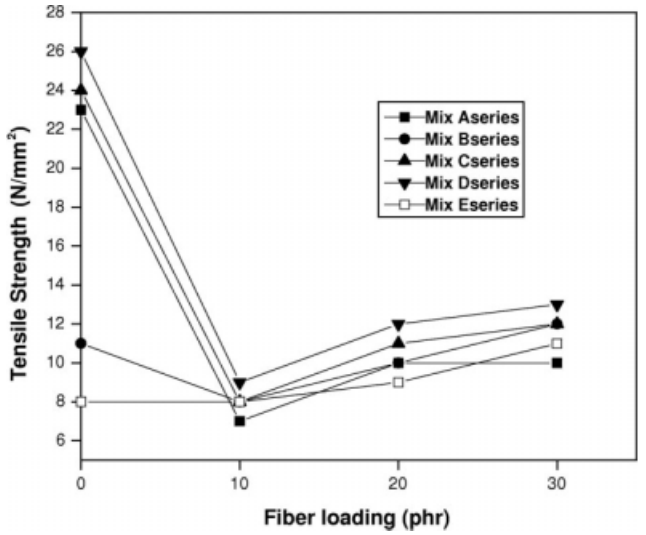

Figure 6 Variation of tensile strength with fiber loading in transverse direction.

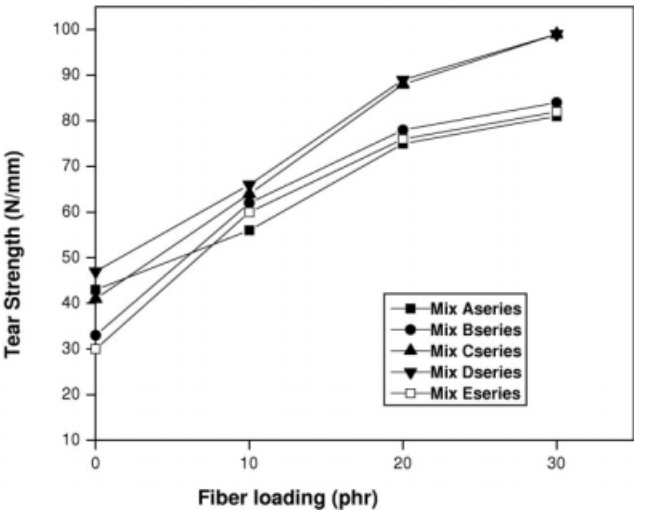

Figure 8 Variation of tear strength with fiber loading in transverse direction.

strength. The transverse orientation of fibers is not effective in supporting the load as the cracks can propagate easily through the interface.

The variation of tear strength with fiber loading is shown in Figure 7. The tear strength registers a tremendous increase in the presence of short fibers. Tear strength increases from 43 N/mm to 106 N/mm by the addition of 30 phr fiber in the case of Mix A. With nanosilica, the tear strength is further improved consistently for all the mixes. For the series A containing no fiber, there is 12% increase in tear strength in the presence of 6 phr of nanosilica. For the 30 phr fiber loaded samples, the tear strength is improved from 106 to118 N/mm with 6 phr nanosilica. With the conventional silica the corresponding improvement in the tear strength is only to 108 N/mm. For transverse orientation of fibers, the variation of tear strength is shown in Figure 8. The tear strength is improved to 81 N/mm with 30 phr fibers without added nanosilica filler. Incorporation of 6 phr of nanosilica raises the tear strength to 99 N/mm for 30 phr fiber loaded sample. For the gum compound (Series A) the tear is improved by 9% with 9 phr nanosilica. For the commercial silica (Series E), the tear strength is consistently lower than the nanosilica composites.

Figures 9 and 10 show the variation of elongation at break with fiber loading in longitudinal and transverse directions, respectively. In both cases, there is a sudden drop in elongation at break with 10 phr fiber loading and after that it remains more or less constant with increase in fiber loading. With fibers distributed uniformly, the matrix becomes more restrained and hence fracture occurs at lower strains.

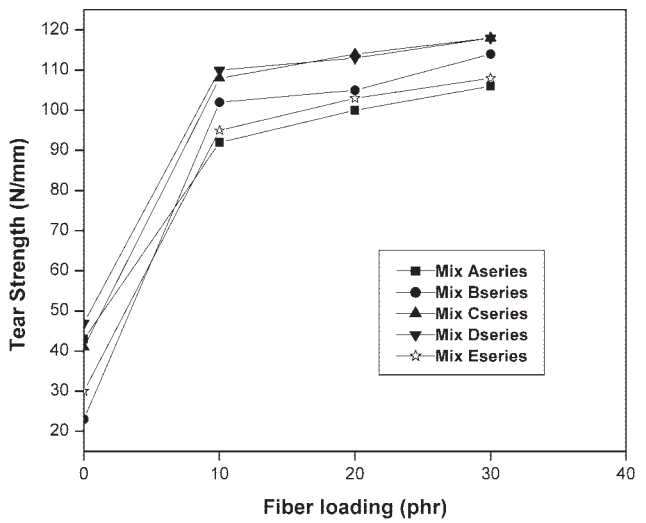

Figure 7 Variation of tear strength with fiber loading in longitudinal direction.

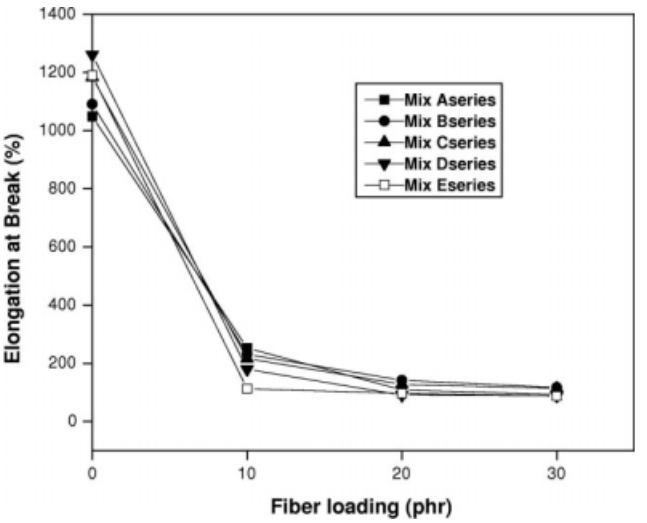

Figure 9 Variation of elongation at break with fiber loading in longitudinal direction.

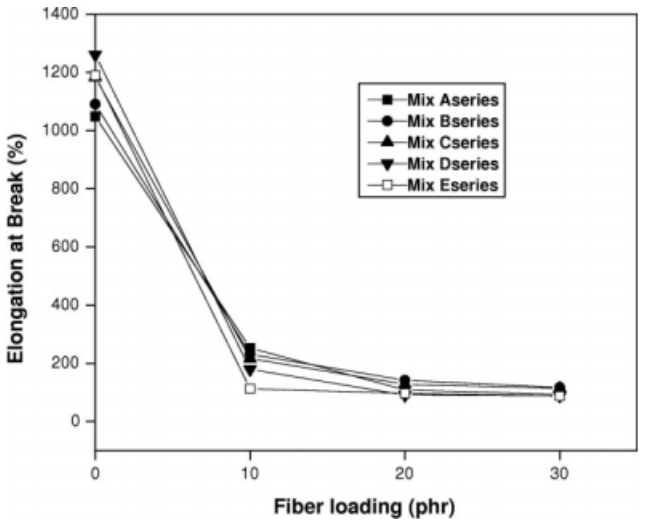

Figure 10 Variation of elongation at break with fiber loading in transverse direction.

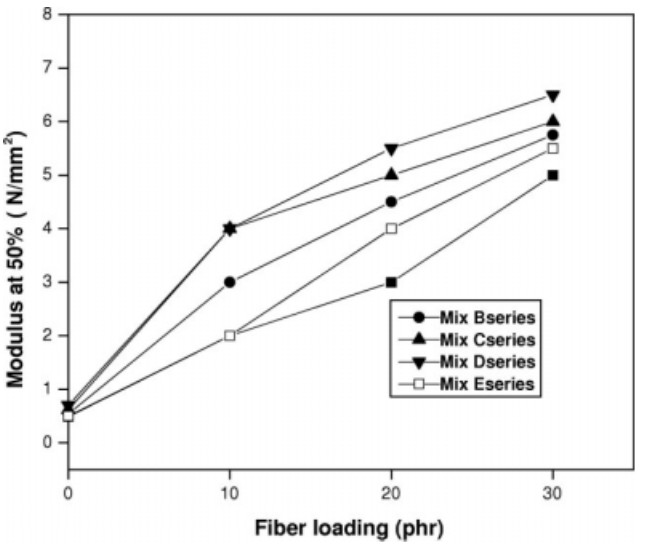

Figure 12 Variation of modulus with fiber loading in transverse direction.

The presence of silica does not seem to have a significant effect on the elongation at break of the fiber filled samples.

The modulus at 50% elongation registers almost linear increase with increasing fiber content. (Fig. 11). There is also significant improvement in modulus values with increasing silica content in the case of fiber filled samples. For the gum compound (Series A0–D0), however, the effect of silica is very limited. By the addition of 9 phr nanosilica, the modulus increases by 55, 33, and 28%, respectively, for 10, 20, and 30 phr fiber loaded samples. It indicates that the silica filler has a significant role in the modulus value of the hybrid composite. The Mixes A_0, B_0, C_0, and D_0 show very low modulus values. The silica improves the modulus only in the presence of fibers. Commercial silica mixes have modulus values lower than that of the mixes containing 3 phr nanosilica. This may due the higher surface area of the lower-particle size nanosilica. Similar trend is also observed in the transverse orientation of fibers (Fig. 12). Here, the observed modulus is much lower than that in the longitudinal direction.

Variation of abrasion loss of the different mixes is shown in Figure 13. There is a drastic fall in the abrasion loss with increasing fiber loading. By the introduction of just 10 phr of fibers, the loss is reduced to approximately 50% in all the cases. With increasing loading of nanosilica, there is a still further reduction in the abrasion loss at any fiber loading, the effect being less prominent at higher fiber contents. For the zero-fiber samples the loss is reduced

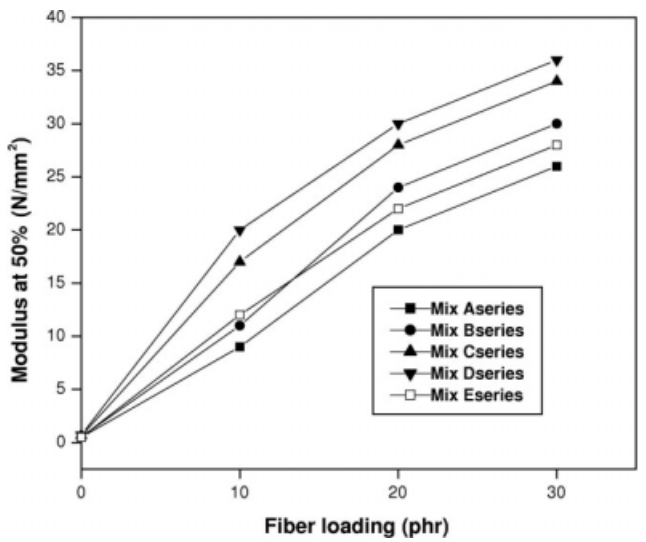

Figure 11 Variation of modulus with fiber loading in longitudinal direction.

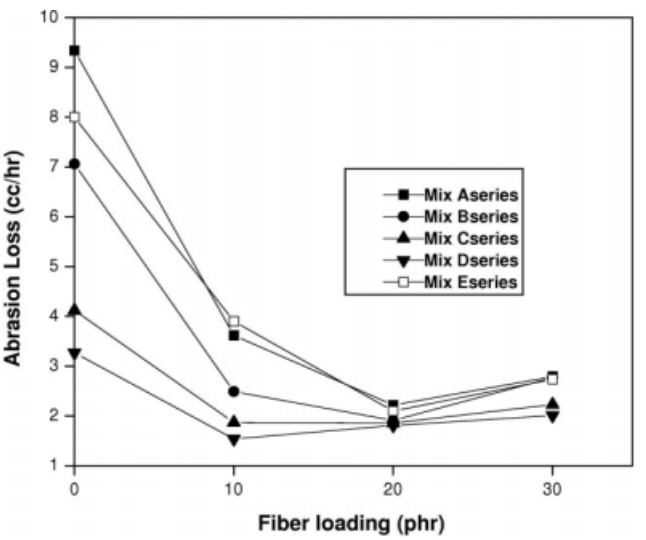

Figure 13 Variation of abrasion loss with fiber loading.

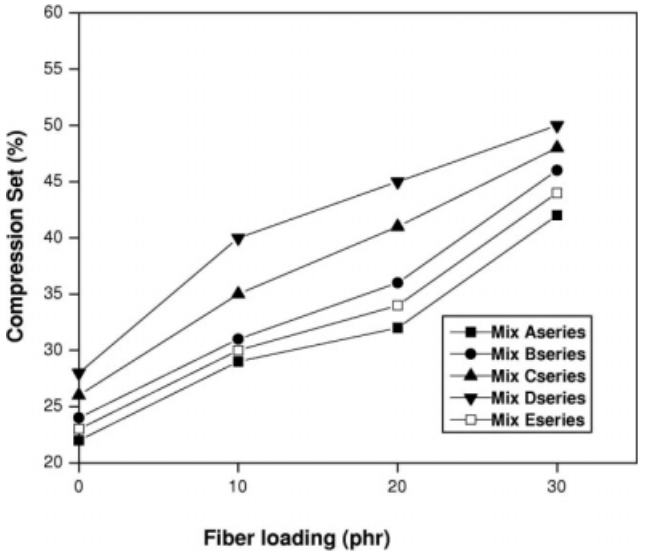

Figure 14 Variation of compression set with fiber loading.

by 123% in the presence of 6 phr of nanosilica(Mixes A_0 and C_0). For the 30 phr fiber loaded samples, the corresponding reduction is only 36% (Mixes A_{30} and C_{30}). Because the matrix along with fiber is abraded out during an abrasion test condition, the effect of silica becomes less significant in the case of fiber loaded samples. The composites containing commercial silica (Series E) show an abrasion loss almost equal to that of gum matrix, which is significantly higher than that of the nanosilica series. A softer matrix has higher abrasion loss. In the case of commercial silica, the weak interface renders the matrix softer and increases the abrasion loss.

Figure 14 shows the compression set of different mixes. Compression set increases with silica content and fiber loading. By the addition of 9 phr silica to

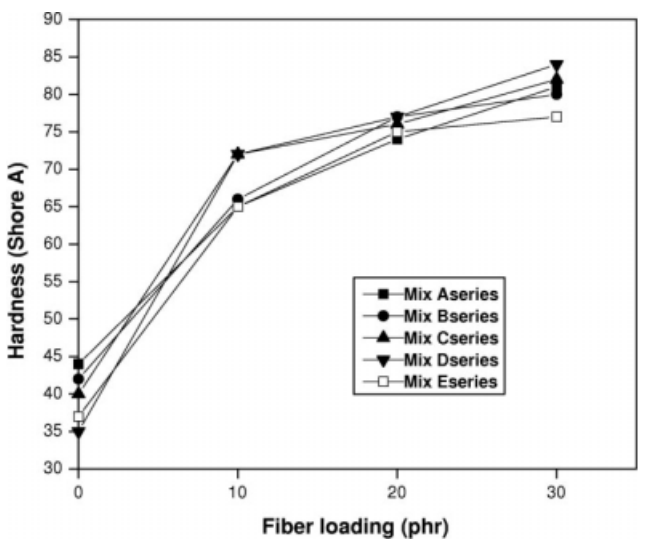

Figure 15 Variation of hardness with fiber loading.

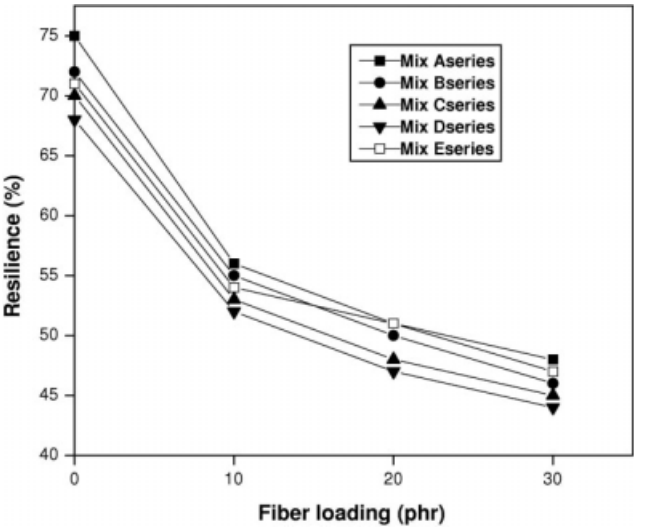

Figure 16 Variation of resilience with fiber loading.

the zero fiber loaded samples (Mixes A_0–D_0), the compression set is increased to 27%. In the case of 30 phr fiber filled samples (Mix D_{30}), the set is increased by 57%. In the presence of reinforcing fillers, the viscoelastic dissipation of energy at the filler-matrix interface is increased. At the elevated temperature of compression test, the matrix becomes soft and undergoes irreversible flow resulting in incomplete recovery on removal of the applied stress. This gives rise to higher compression set values in the case of reinforced matrices. In the presence of the nanosilica, the reinforcement is further enhanced and hence the viscoelastic dissipation is also more. This gives rise to higher compression set in the case of nanosilica composites. Hardness, as expected, is higher for the fiber-filled samples (Fig. 15). With nanosilica the hardness is further enhanced at all fiber loadings. The resilience, an indication of the material elasticity, decreases with fiber content and silica content for all the mixes, as expected (Fig. 16). Resilience shows a reduction from 75% at 0 phr fiber loading to 48% at 30 phr fiber loading (Series A). With increasing silica content, the resilience is further reduced. With 9 phr nanosilica, the resilience of the nonfiber samples is reduced by 12% where as for the 30 phr fiber loaded samples it is lowered by 18%. The dissipation of energy at the fiber-matrix interface results in lower resilience of the composites. With a lesser reinforcing commercial silica, the reduction in resilience is only marginal.

Volume fraction of rubber, V_r

Volume fraction of rubber V_r is a measure of the extent of the crosslink formation and the filler-matrix interaction. A tightly crosslinked/reinforced matrix is expected to swell very minimum in a good

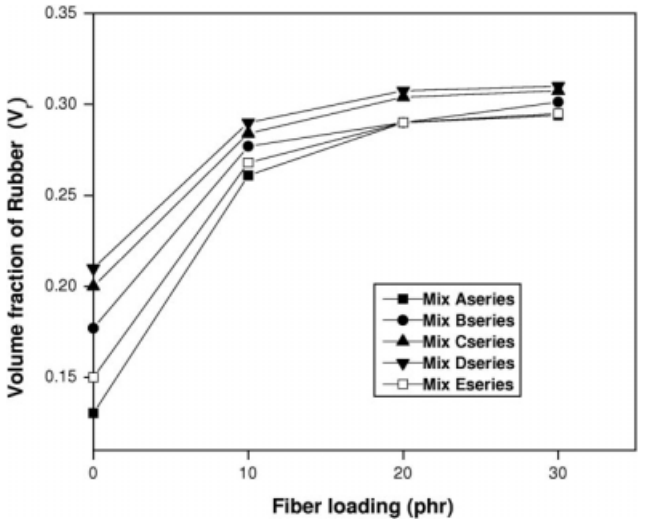

Figure 17 Variation of volume fraction of rubber with fiber loading.

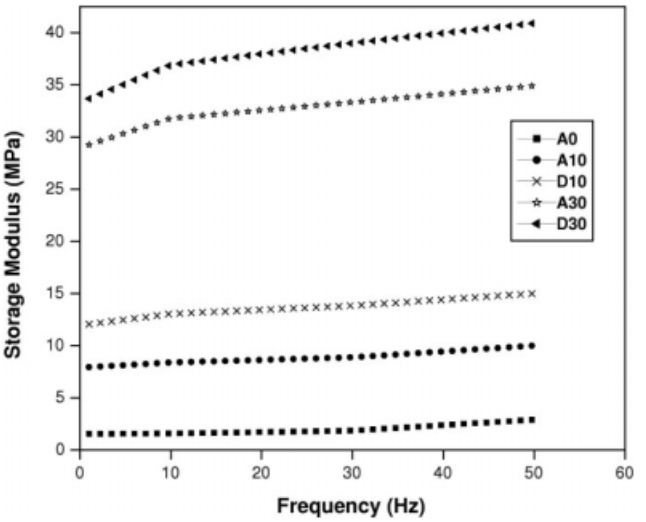

Figure 18 Variation of storage modulus (E′) with frequency.

solvent and hence to have high V_r values as the solvent fails to diffuse through the bulk. Volume fraction, V_r, is found to increase with fiber loading and silica content, as expected (Fig. 17). In the presence of these fillers, the matrix gets more restrained and the diffusion of the solvent becomes limited. This is also evident from the mechanical properties of the composite. The improvement in mechanical properties of the composite with fiber and silica may be attributed to better filler-matrix interaction. V_r of the nanosilica-containing mixes is higher than that of commercial silica composites. This may be arising from the fact that nanosilica can interact better with the matrix because of their higher surface area.

Thermal analysis

Table III gives the thermal degradation characteristics of the Mixes A_o, A_{10}, A_{30}, D_{10}, D_{30}, and E_{30}. All the nanosilica composites show improved thermal stability. Temperature of initiation of degradation increases with silica content, for all the mixes. There is not much change in peak degradation temperature for all the mixes. In presence of 9 phr silica, the temperature of initiation increases from 315 to 324°C for 10 phr fiber loaded sample and for 30 phr fiber loaded samples it increases from 320 to 329°C. The peak rate of decomposition decreases with silica content and fiber content. The peak rate of decomposition decreases from 1.40% to 1.21%/°C by the addition of 9 phr nanosilica (Mix D). This indicates that the material becomes thermally more stable by the addition of nanosilica. In the Mix E_{30}, i.e., the mix containing commercial silica, the temperature of initiation (304°C) and peak degradation temperature (382°C) are lower than other mixes and the peak rate of decomposition is high. i.e.,1.30%/°C.

TABLE III
Thermal Degradation Characteristic of the Mixes

Sample	Temperature of initiation (°C)	Peak degradation temperature (°C)	Peak rate of decomposition (%/°C)
Mix Ao	314	388	1.44
Mix A_{10}	315	387	1.40
Mix D_{10}	324	386	1.21
Mix A_{30}	320	389	1.37
Mix D_{30}	329	387	1.18
MixE_{30}	304	382	1.30

Dynamic mechanical analysis

Figures 18 and 19 show the variation of storage modulus E′ and loss modulus E″ with frequency. Plots A_{10} and D_{10} represent samples containing 10

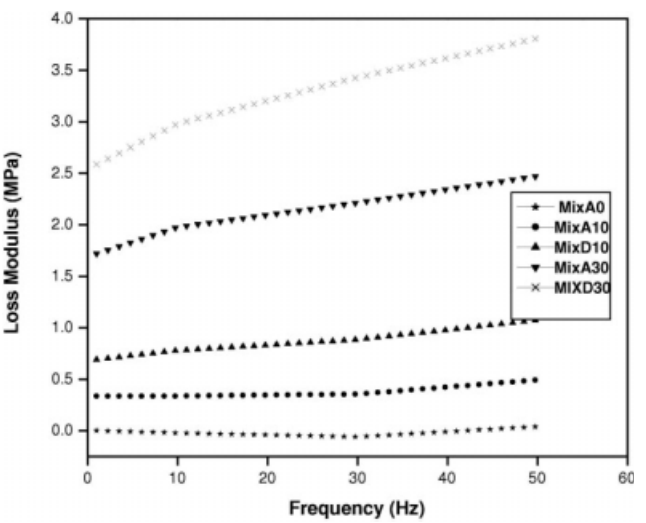

Figure 19 Variation of loss modulus (E″) with frequency.

phr short fibers in the presence of 0 and 9 phr nanosilica, respectively. A_0 is the sample containing no fibers and no silica. E′ and E″ remain almost independent of frequency over the frequency range studied at lower fiber loading (A_{10} and D_{10}) with the silica filled samples showing consistently higher modulus. For the 30 phr fiber loaded (A_{30}) the plots show two distinct regions. Up to 10 Hz, both the modulii show steeper increase. Beyond 10 Hz, the plots are flat. With additional 9 phr silica (D_{30}), though the modulus is increased, the trend is not changed. The two stage frequency dependence of the dynamic modulus may be attributed to the break down of the fiber-matrix interfacial bond under the dynamic deformation conditions during the initial stages of the test. That such a pattern is not apparent in the case of A_{10} and D_{10} indicates that the contribution of the interfacial bond strength is limited in these cases. This is in agreement with the observed trend in the case of tensile strength where the 10 phr fiber loaded samples showed tensile strength lower than the gum compound.

CONCLUSIONS

Nanosilica could be successfully prepared by acid hydrolysis method. The synthesized silica was found have a particle size of 13 nm and a surface area of 295 m^2/g. The nanosilica can be used in natural rubber/short Nylon 6 fiber composite as a component of HRH dry bonding system and also as a filler. The efficiency of HRH dry bonding system is improved in the presence of nanosilica. The nanosilica improves the interfacial bonding between the fiber and the matrix better than the commercial silica. Mechanical properties are improved using the nanosilica in HRH bonding system. The tensile strength, modulus and tear strength are better than the conventional silica. Abrasion resistance and hardness are also better for the nanosilica composites. Resilience and compression set are adversely affected. The composites show anisotropy in mechanical properties. Volume fraction of rubber in a solvent-swollen sample increases with nanosilica. The thermal stability of the composite is also improved in the presence of nanosilica compared with that of the composite containing commercial silica. The storage modulus and loss modulus show two-stage dependence on frequency at higher fiber loading.

References

1. O'Connor, J. E. Rubber Chem Technol 1977, 50, 945.
2. Goettler, L. A.; Shen, K. S., Rubber Chem Technol 1983, 56, 619.
3. Moghe, S. R. Short fiber reinforcement of Elastomers; Amer Chem Soc Rubber Div Meeting, Chicago IL; Oct. 5, 1982, paper No. 20.
4. Prasanthakumar, R.; Sabu Thomas, J. Adhe Sci Technol 2004, 15, 633.
5. Ogi, K.; Nishikawa, T.; Okano, Y.; Taketa, I. J Adv Compos Mater 2007, 16, 181.
6. Abdelmouleh, M.; Boufi, S.; Belgacem, M. N.; Dufreshe, A. Compos Sci Technol 2007, 67, 1627.
7. Kondo, A. Setchaku, 1978, 22, 135.
8. Rajeev, R. S.; Bhowmick, A. K.; De, S. K.; Bandyopadhyay, S. J. Appl Polym Sci 2003, 90, 544.
9. Suhara, F.; Kutty, S. K. N.; Nando, G. B. Polym Plast Technol Eng 1998, 37, 241.
10. Chunxiang Y. Y.; Xiaolei L.; Xinkui, S.; Wang.J Mater Sci 2007, 42, 6347.
11. Sreeja, T. D.; Kutty, S. K. N. Polym Plast Technol Eng 2002, 41, 77.
12. Seema, A.; Kutty, S. K. N. Polym Plast Technol Eng 2005, 44, 1139.
13. Gahara, In Synthetic Fiber Materials; Brody, H., Ed.; Longman: Harlow U.K., 1994, p 239.
14. Kutty, S. K. N.; Chaki, T. K.; Nando, G. B. Polym Degrad Stab 1992, 38, 187.
15. Suhara, F.; Kutty, S. K. N.; Nando, G. B. Polym Degrad Stab 1998, 61, 9.
16. Seema, A.; Kutty, S. K. N. J Appl Polym Sci 2006, 99, 532.
17. Seema, A.; Kutty, S. K. N. J Polym Mater 2006, 55, 25.
18. Dunnom, D. D. Hi-Sil Bulletin; PPG Ind., 1967, No.35.
19. Derringer, G. C. J Elastoplast 1999, 3, 230.
20. Murty, V. M.; De, S. K. Polym Eng 1984, 4, 313.
21. Rajeev, R. S.; De, S. K.; Bhowmick, A. K. J Mater Sci 2001, 36, 2621.
22. Murty, V. M.; De, S. K.; Bhagawan, S. S.; Sivaramakrishnan, R.; Athithan, S. K. J Appl Polym Sci 1983, 28, 3485.
23. Ismail, M. N.; Ghoneim, A. M. Polym Plast Technol Eng 1999, 38, 78.
24. Geethamma, V. G.; Mathew, K. T.; Lakshminarayanan, R.; Thomas, S. Polymer 1998, 39, 1483.
25. Tapasikotoky; Dolui, S. K. J Sol Gel Sci Technol 2004, 20, 107.
26. Chrusoid, J.; Slusaraski, L. Mater Sci 2003, 21, 461
27. Sreeja, T. D.; Kutty, S. K. N. Polym Plast Technol Eng 2003, 42, 239.
28. Murty, V. M.; De, S. K. Rubber ChemTechnol 1982, 55, 287.